

An Information-Theoretic Comparison Between Coherent and IM/DD Transmissions for Free Space Optical Communications

Ayman Zahr¹, Graduate Student Member, IEEE, Giulio Colavolpe², Senior Member, IEEE, Tommaso Foggi², Balázs Matuz, Senior Member, IEEE, and Armando Vannucci²

Abstract— We investigate the performance of free-space optical communication systems in the presence of atmospheric turbulence to assess the advantages that a coherent communication system can bring with respect to a conventional intensity modulation and direct detection (IM/DD) system. The perspective is an information-theoretic one, hence we evaluate the mutual information and the corresponding outage probability of both channels, with various traditional symbol constellations, as a pragmatic approximation to the capacity, or to the outage capacity, of those channels. In addition, we analyze non-uniform symbol constellations to evaluate the possible shaping gain that can be achieved under different channel conditions. We propose a method to quantify the gain that the coherent solution can achieve, in terms of signal-to-noise ratio (SNR), so that it can be compared, on a techno-economical basis, against the higher cost that it implies.

Index Terms—Free-space optics, atmospheric turbulence, coherent optical systems, IM/DD systems, shaping gain.

I. INTRODUCTION

FREE-SPACE optical (FSO) systems, like early fiber optic communication systems, have traditionally resorted to intensity modulation and direct detection (IM/DD) techniques, both for indoor communications [1] and for low Earth orbit (LEO) satellite-to-ground links [2], [3]. Despite the great potential of coherent transceiver technology, nowadays a standard in optical fiber systems, this is neither a widespread nor a totally mature technology for the space-to-ground commu-

nications scenario.¹ Moreover, information-theoretic studies on FSO communication systems are essentially limited to the IM/DD case. For instance, the capacity of IM/DD FSO systems has been investigated in [6] in the presence of randomly time-varying channels while, to our knowledge, such a study has never been carried out for coherent FSO links.

The tools of information theory such as, e.g., the computation of the capacity (or of the outage capacity) are the only ones that can assess the ultimate performance of a transmission system. Hence, an information-theoretic comparison between a coherent and an IM/DD system, which represent profoundly different technological solutions for FSO communications, is meaningful in view of the deployment of the two technologies. This is the focus of our work. We resort to physical channel models that have already been introduced, in the existing literature on FSO links, and that justify the analytical communication system models on which the evaluation of the capacity is based.

For a LEO satellite-to-ground link, the presence of atmospheric turbulence is considered to be the principal impairment. Turbulence distorts the optical field so that its wavefront should be, at least partially, recovered by adaptive optics (AO) systems before entering the ground telescope [7]. Still, the received power is eventually attenuated by *optical scintillation* [8], that can be modelled by a lognormal or by a gamma-gamma distribution [9]. Given the long coherence time of scintillation and of the possibly residual phase distortions, typically in the order of milliseconds [7], compared to the duration of transmitted codewords, a block-fading model is appropriate for the Free-space optical (FSO) channel, unless a long interleaver is adopted, which is often considered to be impractical [6]. As a consequence, under the block-fading hypothesis, *outage capacity* should be considered as the appropriate metric to characterize the channel.

¹To our knowledge, at least two coherent FSO communications systems have been recently demonstrated by NASA. One is TBIRD (terabyte infrared delivery) [4], that reaches a considerable data-rate of 200 Gbps with a LEO cubesat and, notably, includes a commercial fiber telecom transceiver and EDFA. The other is planned within the Artemis II (Moon-to-Mars) missions, that will employ an *Orion Artemis-II Optical Communications* (O2O) terminal that includes a coherent FSO system for the high-rate (5 Gbps) trunk line between Earth and the Moon, namely the currently deployed LCRD (laser communications relay demonstration) ground receiver, which has coherent FSO communication capabilities [5].

Manuscript received 14 July 2023; revised 19 January 2024; accepted 20 January 2024. Date of publication 14 February 2024; date of current version 9 May 2024. This work was supported in part by the European Space Agency (ESA) funded activity SatNEx V COO2 WI 2.3 “Fibre optics techniques for future free-space optical satellite communications” and in part by the University of Parma through the action Bando di Ateneo 2022 per la ricerca co-funded by MUR -Italian Ministry of Universities and Research under Grant D.M. 737/2021-PNR-PNRR-NextGenerationEU. (Corresponding author: Armando Vannucci.)

Ayman Zahr and Balázs Matuz are with the Institute of Communications and Navigation, German Aerospace Center (DLR), 82234 Weßling, Germany (e-mail: ayman.zahr@dlr.de; balazs.matuz@tum.de).

Giulio Colavolpe, Tommaso Foggi, and Armando Vannucci are with the Department of Engineering and Architecture, University of Parma, 43124 Parma, Italy (e-mail: giulio@unipr.it; tommaso.foggi@unipr.it; armando.vannucci@unipr.it).

Color versions of one or more figures in this article are available at <https://doi.org/10.1109/JSAC.2024.3365898>.

Digital Object Identifier 10.1109/JSAC.2024.3365898

For IM/DD optical transmission systems, the symbol constellation belongs to \mathbb{R}^+ , i.e., only real and positive light intensities are allowed. The channel capacity of such a FSO intensity modulated system has been studied in the literature. In [6], the capacity-achieving non-uniform input signal distribution is evaluated considering constraints on the average intensity as well as on the peak optical power, showing that substantial performance improvements can be achieved by a proper shaping of the symbol constellation.

The adoption of coherent transceivers for FSO communications opens up the field of investigation to similar analyses, performed on a different channel model, where a general complex optical field, i.e., belonging to \mathbb{C} and with signed components, carries the information [10], enlarging the signal space by a factor of two. A further doubling of the signal space is provided by the possibility to exploit polarization division multiplexing, with coherent transceivers, thus yielding a factor of four for the overall enlargement of the signal space. Albeit, for the sake of simplicity, we shall restrict our attention on the in-phase (i.e., real) component of the complex optical field envelope and neglect the multiplexing gain brought about by dual-polarization transmission.

In this work, we explore a comparison between IM/DD solutions and a coherent transceiver for FSO transmission over a LEO satellite-to-ground link, by means of mutual information and related system outage probabilities, for practical signal constellations. In order to keep the analysis at an affordable level, we refer to simple cases where the transmission channel can be modelled as an additive Gaussian channel with fading due to optical scintillation. Thus, we neglect the effects of optical shot noise as well as the effect of the residual phase noise after the AO correction, that can be attributed to the turbulent piston mode (not corrected by traditional AO systems).

Different receivers employing different technological solutions imply different noise figures, besides different costs, that cannot be directly compared. We briefly summarize the different sources of noise for optical systems, along with their impact on SNR, in Appendix A. Given that the average transmitted power for satellite communications is generally a scarce resource, we adopt it as the main term of comparison for both kinds of systems, leaving the additive noise level as an extra variable that should be separately evaluated on a techno-economical basis. However, we shall provide some values of practical interest, for the noise power and the link budget, to directly compare the performance achieved by an IM/DD system versus that of a coherent system. The effect of optical scintillation shall be modelled as a lognormal variable, which is considered accurate in the present case of moderate atmospheric turbulence. In the presence of more severe scintillation conditions, the analysis can be easily extended to account for different statistical distributions, like, e.g., the gamma-gamma [9]. Reducing the atmospheric turbulence phenomenon to optical scintillation-induced fading, as we assume here, relies on the role of the AO subsystem, whose specific operation and efficacy are discussed in other works, like [7]. Hence, if the turbulence conditions are so critical as to impair the operation of the AO, then different models

and analyses are required; however, this is rarely the case, as demonstrated in [7].

The paper is organized as follows. In Sec. II we describe the architecture of the systems that we consider and derive their corresponding analytical models. The performance that can be obtained from the two types of systems is quantified in Sec. III in terms of information rate, under various channel conditions and with different modulation schemes, as a function of the average transmitted optical power. The performance comparison is extended in Sec. IV to include the effects of link budget and noise, that stems from different physical sources for the two systems. Finally, conclusions are drawn in Sec. V, along with hints for future research directions.

II. SYSTEM MODEL

In order to compare FSO transmission systems of different nature, such as those employing a coherent or an IM/DD transceiver, different system models are analyzed to evaluate the achievable mutual information for given input signal statistics that obey some prescribed constraints. In both cases, the physical channel, i.e., the transmission medium, is the same and is assumed to suffer only from the atmospheric turbulence effect, which introduces a random fading that is frequency flat across the transmission bandwidth. Atmospheric turbulence is a complicated phenomenon with a rich scientific literature [8], whose effects are often reduced to scintillation-induced fading, in the context of digital communications [1], [7], [9], [11], so as to adopt simple and reliable communication channel models that are easy to implement in simulations as well as tractable for the analysis. The only other impairment is additive white Gaussian noise (AWGN) that may be due to different physical sources, such as an amplified spontaneous emission (ASE) noise source introduced at the optical amplification stage in the front-end of a coherent receiver, or due to thermal noise introduced at the transimpedance amplifier (TIA) stage that follows the avalanche photodiode (APD) for the intensity detection of modulated light, plus possible ambient light-induced shot noise.

A. Intensity Modulation and Direct Detection System

The optical transmission system architecture that is expected to require less resources and, therefore, to exhibit a worse performance is the traditional solution based on intensity modulation at the transmitter side and direct detection of the received light power at the receiver side. Despite being the oldest solution adopted in optical communications, it is still widespread nowadays for short-reach fiber links and/or when cost constraints make it preferable, compared to more costly and performing solutions. This is the case, e.g., in data-center interconnects (DCIs), which make up a significant fraction of the global fiber-optic network [12]. Despite FSO satellite-to-ground links having little to share with DCIs, the long-lasting history of IM/DD systems turns out to be a positive factor in terms of robustness and reliability in space applications.

The receiver that we shall investigate in the present case is a very simple and traditional one, consisting of an APD at the front-end for opto-electronic conversion, followed by a TIA,

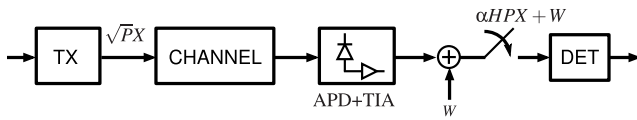


Fig. 1. Schematic of the IM/DD transmission system. TX: transmitter; APD+TIA: avalanche photo-diode plus transimpedance amplifier; DET: detector.

that introduces extra thermal noise. We shall assume, however, that the APD excess noise factor is small enough to make shot noise negligible compared to thermal noise, so that the TIA is the dominant source of noise. Thus, a traditional AWGN model applies to the system, as in [6], where the additive Gaussian noise is independent of the received signal. In the absence of intersymbol interference, the very simple discrete-time channel model that characterizes the IM/DD system is thus

$$Y = \alpha H P X + W \quad (1)$$

where $P > 0$ is the parameter that drives the transmitted optical power and $X \in \mathbb{R}^+$ is the transmitted symbol, belonging to a given constellation, whereas $H \sim p_H(h)$ is the random fading of the light intensity that is due to atmospheric turbulence and that is known as optical scintillation. The parameter α represents the power attenuation due to path loss and to any other constant loss factor that can be computed from the link budget, as detailed in Sec. IV. Hence, the received light intensity in the absence of fading and noise is $\alpha P X$, which is in turn equal to the photodetected current. In (1), $W \sim \mathcal{N}(0, \sigma_W^2)$ is the zero-mean real AWGN with normal distribution and variance σ_W^2 that stems from thermal noise samples, as generated by the receiver TIA, so that its variance is the one reported in Appendix A, where we discuss the sources of noise in optical receivers. In particular, it is $\sigma_W^2 = \sigma_T^2$, whose expression is given in (26). Fig. 1 shows a diagram of the IM/DD system.

The received electrical signal $Y \in \mathbb{R}$ in (1) is thus real and the electrical SNR, for a realization h of the scintillation is

$$\text{SNR}_{\text{IM/DD}}(h) = \alpha^2 h^2 \frac{P^2 E[X^2]}{\sigma_W^2} = \alpha^2 h^2 \frac{(PE[X])^2 K^2}{\sigma_W^2} \quad (2)$$

where $(PE[X])$ is the average transmitted optical power and

$$K = \frac{\sqrt{E[X^2]}}{E[X]} \quad (3)$$

defines a constellation-dependent factor that is equal to the ratio between the root mean square and the average symbol value.

The presence of P^2 in (2) should not surprise since P is related to the optical power, which is proportional to the photodetected electric current, whose power is in turn proportional to the electrical SNR.² In fact, it is the electrical SNR in (2) that dictates system performance and that is the main figure on which the bit error rate (BER), as well as the mutual information, can be evaluated. It is worth noting

²We assume, without loss of generality, that the responsivity of the photodiode providing the opto-electronic conversion is 1 [A/W].

that in a number of previous works on IM/DD systems, the SNR is defined in different ways, where the square of the mean of X appears instead of the mean-square signal value.³ Nevertheless, citing [1], “The signal-to-noise ratio (SNR) of a direct-detection receiver is proportional to the square of the received optical power”, so that [1] employs the definition (using our symbols) $\text{SNR}(h) = \alpha^2 h^2 P^2 E[X]^2 / \sigma_W^2$, hence using the square of the received (average) optical power, which, in addition, facilitates comparison among different systems.

As long as the transmitted optical power PX in (1) follows a discrete multilevel distribution, it is possible to express the mean-square value in (2) through the square of the average, $E[X]^2$, adopted in [6] and [1]. This is true even in the presence of a probabilistic shaping of the constellations, so that we defined K in (3) for this purpose. For instance, for on-off keying (OOK) modulation, where the optical power is either zero or the peak value A , with possibly non-uniform symbol probabilities, we obtain $K^2 = 1/\text{Pr}(A)$. It is thus clear that, for a given average transmitted optical power ($PE[X]$), a probabilistic shaping of the transmitted constellation has a direct impact on the electrical SNR in (2), on which the performance depends. This is of course no longer true when X is a signed random variable, with possible zero mean.

In (2), we choose to adopt a viewpoint that emphasizes the electrical signal power occurring after the opto-electronic conversion. Therefore, for the purpose of system comparison that will follow, we should keep in mind that different SNR values result, from the same average optical power, when modulations employing different symbol constellations are adopted.

B. Coherent Transmission System

For a coherent FSO transmission system, it is the complex optical field envelope $X \in \mathbb{C}$ that is detected by the so-called *90°-hybrid* optical circuit, that is at the core of a coherent transceiver [13]. The two couples of *balanced photodetectors* that follow allow the detection of the in-phase and quadrature components of X as it usually occurs in radio frequency communications. The beating of the signal with a local oscillator⁴ yields the real and imaginary parts of the complex envelope X of the light field, so that two-dimensional modulation schemes, such as QAM or PSK (for uniformly distributed signals), are affordable. Typically, the polarization of light is exploited as a further dimension to multiplex signals with orthogonal states of polarization, thus increasing the information-bearing capacity of the FSO channel by a factor of two. In the numerical results that follow, for ease of presentation we will only consider the in-phase component of a single polarized signal and will not include the other dimensions that might however straightforwardly be accounted for.

³For instance, in [6] the same system model as (1) is considered, whereas the SNR is defined (using our symbols) as $\text{SNR}(h) = \alpha h P E[X] / \sigma_W$, i.e., resorting to the average optical power.

⁴Although the local oscillator might not be perfectly tuned to the optical carrier frequency and might not at all be locked to the carrier phase, we can conceptually refer to the coherent receiver as a classic homodyne receiver scheme.

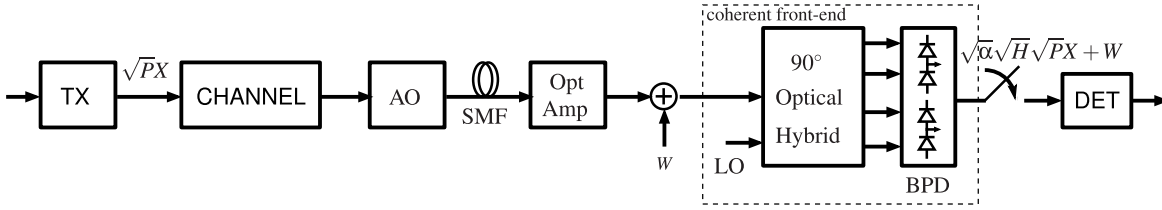


Fig. 2. Schematic of the coherent transmission system. TX: transmitter; AO: adaptive optics; SMF: single-mode (coupling) fiber; Opt Amp: optical amplifier; LO: local oscillator; BPD: balanced photodetectors; DET: detector.

The discrete-time channel model, after analog-to-digital (A/D) conversion, is

$$Y = \sqrt{\alpha}\sqrt{H}\sqrt{P}X + W \quad (4)$$

where, similarly to (1), the parameter $P > 0$ drives the transmitted optical power and $X \in \mathbb{C}$ is the complex transmitted symbol, belonging to a two-dimensional constellation, so that $\sqrt{P}X$ is the complex envelope of the transmitted optical field. Being H the optical scintillation, i.e., the random power attenuation affecting the transmitted optical intensity, equal to $P|X|^2$, the random amplitude attenuation is its square root, as appears in (4). Similarly, $\sqrt{\alpha}$ includes the non-random amplitude attenuation factors coming from the link budget (see Sec. IV). Finally, $W \sim \mathcal{CN}(0, \sigma_W^2)$ is the complex normal zero-mean AWGN with variance $\sigma_W^2/2$ per component that affects the received signal samples. Fig. 2 shows a diagram of the coherent transmission system.

The effects of atmospheric turbulence on the complex optical field induce a phase response too, so that the model in (4) can appear to be oversimplified. However, the phase impact of turbulence can be mitigated either by using channel matched array receivers, which comprise multiple subapertures [11], or otherwise by using a single-aperture receiver with AO to correct wavefront distortion. This is the solution that we assume here, also considered in [5], and analyzed in detail in [7]. To summarize, the impact of atmospheric turbulence on the transmitted optical signal is such that the local phase distortions disrupt the wavefront of the input field on ground, resulting in a speckle pattern across the telescope pupil plane.⁵ An adaptive optics subsystem, reported in Fig. 2, is thus necessary to equalize the wavefront prior to mixing the received field with the local oscillator, in the 90°-hybrid, so as to maximize their *coupling efficiency*, hence the photodetected signal. In [7], a detailed and complete simulator is employed to evaluate the complex space- and time-varying channel response due to atmospheric turbulence, accounting for the different optical rays in the received lightwave beam (which implies physically faithful but long simulations). As demonstrated in [7], most of the residual phase variations after the AO correction can be attributed to an effect called *atmospheric piston* [14], that it is not corrected by traditional AO systems. Nevertheless, such kind of phase changes due to the atmosphere are relatively stable and it is reasonable to consider them as a quasi-constant phase, that can be included

⁵Unless the telescope is small enough, in which case the AO system is not necessary: the limiting dimension for the telescope's diameter is the so called *Fried parameter*, that is one of the physical parameters characterizing atmospheric turbulence.

in the model of a non-ideal local oscillator which however is not considered in (4).

The average transmitted optical power, for the coherent channel model, is $PE[|X|^2]$. The SNR obtained from (4) for a given value $H = \bar{h}$ of the scintillation is

$$\text{SNR}_{\text{coh}}(h) = \alpha h \frac{PE[|X|^2]}{\sigma_W^2} \quad (5)$$

resulting in an expression that significantly differs from the corresponding one for the IM/DD case in (2).

Different receiver architectures could be envisaged to implement a coherent transmission link. However, since the coherent format is not a consolidated choice but rather a novel solution for FSO systems, we refer to the architecture that is most commonly adopted in coherent fiber-optic links, consisting in the cascade of an optical amplifier followed by the proper coherent receiver, made of a 90°-hybrid and of the balanced photodetectors [13]. The optical amplifier, usually with a large gain, brings the (weak) received optical signal to a sufficient optical power level that allows an effective opto-electronic (O/E) conversion, at the coherent receiver front-end, that is not impaired by severe shot noise. Within this scenario, it is reasonable to assume that the dominant source of noise is the ASE that spontaneously arises in the preamplifier and that adds to the useful signal before the O/E conversion, so that the electrical SNR is the one reported in (41). As detailed in Appendix A, the corresponding noise variance is $\sigma_W^2 = \sigma_{\text{ASE}}^2/(2G) = n_{\text{sp}}\hbar\nu_0(1 - 1/G)\Delta f$, where the total ASE noise variance (40) is considered at the amplifier input and divided by 2 to account only for the noise component that is co-polarized with the signal.

Thus, besides representing a traditional solution in fiber optic systems, the optically preamplified coherent receiver is consistent with the additive Gaussian channel model in (4).

C. Statistics of Scintillation

We assume a lognormal distribution for the scintillation H , i.e., $H \sim \mathcal{LN}(\mu_N, \sigma_N^2)$, with probability density function (pdf)

$$p_H(h) = \frac{1}{h\sqrt{2\pi\sigma_N^2}} \exp\left\{-\frac{(\ln(h) - \mu_N)^2}{2\sigma_N^2}\right\}, \quad (6)$$

with mean and variance

$$\mu_H = \exp\{\mu_N + \sigma_N^2/2\} \quad (7)$$

$$\sigma_H^2 = \exp\{2\mu_N + \sigma_N^2\} (\exp\{\sigma_N^2\} - 1) \quad (8)$$

The strength of the optical scintillation phenomenon is usually characterized by the power scintillation index (PSI), defined as the normalized variance of the received intensity, whose expression is thus

$$S \triangleq \frac{E[H^2]}{E[H]^2} - 1 = \frac{\sigma_H^2}{\mu_H^2} = \exp\{\sigma_N^2\} - 1 \quad (9)$$

which depends uniquely on σ_N^2 and not on μ_N .

A lognormal distribution for the scintillation parameter H is considered accurate at low to moderate scintillation indices values, e.g., when S is in the order of 0.1, a value corresponding to a 10° elevation for a satellite transmitting at 847 nm lightwave carrier, or to a 18° elevation for a satellite transmitting in the ‘third window’ at 1550 nm [10]. When more severe atmospheric conditions imply larger values of S , e.g., in the order of 1.0, then other distributions like the gamma-gamma or the K-distributions are considered more accurate [9].

The pdf in (6) has the feature that any power of H , including its square root or its inverse, is lognormal too. This is a consequence of the well known property that a linear transformation of a normal variable is again normal (with proper shifting of the mean and scaling of the variance). Since, by the definition of a lognormal variable H , it is $H = \exp(N)$, for some normal variable $N \sim \mathcal{N}(\mu_N, \sigma_N^2)$, then a linear transformation $N \rightarrow aN + b$ results in a corresponding transformation $H \rightarrow \exp(aN + b) = e^b H^a$, i.e., in a multiplication and a power transformation of the original lognormal variable. As a result, \sqrt{H} in (4) has a pdf similar to H in (1), except for a modification of its mean and variance.

D. Comparison of IM/DD and Coherent Systems

It is evident that the two kinds of systems described in Sec. II-A and Sec. II-B are totally different, both in the transmission strategy and in the receiver architecture. Albeit, both have been modelled, under proper technological constraints, by a classical additive Gaussian memoryless channel, that is relatively easy to analyze. In optical communications, the Gaussian memoryless channel has often been used as an auxiliary channel to obtain (after a proper matching of system parameters) a lower bound to the capacity of the nonlinear and possibly non-additive noisy fiber optic channel (see, e.g., [15], [16] and references therein).

The two Gaussian memoryless channels that model the system architectures of Secs. II-A and II-B are affected by physically different sources of noise, for which a direct comparison is not feasible. However, we wish to adopt a more general perspective, as done in [17] to account for the profound technological difference between single-core and (few- or) multi-core fibers. In our case, instead, the transmission medium is the same but the transceivers are different. Regarding the two kinds of transmitters, despite they are technologically different, both rely on the transmitted optical power, which is the main scarce resource, on board the satellite. Spacecrafts that fly in LEO must certainly obey less stringent power limits, compared to those flying in much larger distances, since power supply is an increasingly scarce resource as the distance to the spacecraft grows. Nonetheless,

power is a huge and limiting constraint and it is absolutely meaningful to directly compare different solutions to exploit a given average power at the transmitter, which is dictated by the power-supply devices on board of a satellite including solar cells and batteries.

III. CHANNEL CAPACITY AND INFORMATION RATE

Both (1) and (4) represent fading channels with additive Gaussian noise and different input constraints. Ergodic channel capacity of unconstrained input Gaussian fading channels can be computed under the assumption of a sufficiently long interleaver, that is able to average out the impact of the quasi static fading due to scintillation. It is obtained by averaging the capacity $C(h)$ of an AWGN channel given a particular realization $H = h$, under the assumption of Gaussian distributed channel inputs, as

$$C = \int_0^{+\infty} C(h) p_H(h) dh \quad (10)$$

where $C(h)$ is Shannon capacity result for a Gaussian channel

$$C(h) = B \log(1 + SNR(h)). \quad (11)$$

In (11), B is the channel bandwidth, measured in bits per second. Alternatively, one can use the spectral efficiency $\eta = C/B$ [bits/s/Hz], which can account for *time-frequency packing* formats [10]. In (11), the SNR is evaluated for a given value of the scintillation, hence it corresponds to either (2) or (5) for the two system models considered here, while the effective received SNR is its average, e.g., for a coherent system, $SNR = E[SNR(H)] = \mu_H \alpha PE [|X|^2] / \sigma_W^2$.

For practical finite signal constellations, such as amplitude shift keying (ASK) or phase-shift keying (PSK), the achievable rate or mutual information (MI) can be computed as

$$I(X; Y) = \max_{P(x)} \int_0^{+\infty} I(X; Y | H = h) p_H(h) dh. \quad (12)$$

In (12), we average over the conditional mutual information for a given scintillation value $H = h$ and find the input distribution $P(X)$ which maximizes the average rate expression. As it is known, these rates are upper bounded by the actual capacity expression in (10). Resorting to a uniform distribution of the constellation points may yield a further penalty with respect to capacity.

If, instead, the use of a very long interleaver is unfeasible, a block fading channel model is considered to analyze the performance of the FSO links, as in [6]. In these channels, the modulated codeword is partitioned into L blocks, where L is called diversity order of the system. They rely on the assumption that the channel gain H_i is constant over each i -th block of transmission, but independent and identically distributed (i.i.d.) over different blocks. Due to the limited number of realizations of the channel gain, the impact of very low (even zero) channel gains cannot be averaged out, which in our case yields a null Shannon capacity. Hence, such systems inherently assume a probability of failure or outage. One can determine the ϵ -outage capacity, which is the maximum rate that ensures reliable communication for (at least) a fraction of $1 - \epsilon$ of time.

In both systems of interest we assume, without loss of generality, that H is normalized so that its mean value $\mu_H = 1$, i.e., that $\mu_N = -\frac{\sigma_N^2}{2}$ in (7). In the following, we select $\sigma_N^2 = 0.1$, which can be converted to the power scintillation index S as in (9). As discussed in Sec. II-C, this value is typical for atmospheric channels with moderate turbulence.

A. Intensity Modulation and Direct Detection System

For an IM/DD system, we assume, in general, to modulate the transmitted light intensity by a multilevel scheme, which reduces to the OOK modulation in the case of a binary symbol constellation. By resorting to the discrete-time channel model in (1), αHPX is the noiseless received light intensity in the presence of fading.

We impose a normalization of the symbol constellation,

$$E[X] = 1, \quad (13)$$

so that the average transmitted optical power ($PE[X]$) in (2) is P . As a consequence, for a given realization of the scintillation $H = h$, the instantaneous SNR in (2) becomes

$$\text{SNR}_{\text{IM/DD}}(h) = \alpha^2 h^2 \frac{P^2 K^2}{\sigma_W^2}. \quad (14)$$

For an ergodic fading channel the capacity $C_{\text{IM/DD}}$ is

$$C_{\text{IM/DD}} = \max_{P(x)} \int_0^\infty I(X; Y|H = h) p_H(h) dh \quad (15)$$

where the MI $I(X; Y|H = h)$ in (15) corresponds to the MI of an AWGN channel with instantaneous $\text{SNR}_{\text{IM/DD}}(h)$.

For the block fading channels, we first define the outage probability as the probability that the transmission rate R exceeds the average instantaneous MI over L blocks, i.e.,

$$p_{\text{out,IM/DD}}(R) = \Pr \left\{ \max_{P(x)} \frac{1}{L} \sum_{\ell=1}^L I(X, Y, H_\ell) < R \right\} \quad (16)$$

where the random variable (r.v.) $I(X, Y, H_\ell)$ is the rate supported in block ℓ with values $I(X; Y|H_\ell = h)$. The ϵ -outage capacity is the maximum transmission rate such that the outage probability is smaller than a target value ϵ ,

$$C_{\epsilon, \text{IM/DD}} = \underset{R}{\operatorname{argmax}} p_{\text{out,IM/DD}}(R) < \epsilon. \quad (17)$$

In average, error-free communication is possible at a rate

$$\bar{R}_{\epsilon, \text{IM/DD}} = (1 - \epsilon) C_{\epsilon, \text{IM/DD}}. \quad (18)$$

It is worth noting that in the SNR expressions (2) and (14), the square of the scintillation realization h^2 appears for the IM/DD case, whereas h appears for the coherent case (5). As discussed in Sec. II-C, any power of H is still log-normal (LN) distributed, so that, by applying the quadratic transformation of H , it is easy to show that $H^2 \sim \mathcal{LN}(2\mu_N, 4\sigma_N^2)$.

Average rates $\bar{R}_{\epsilon, \text{IM/DD}}$ versus the average transmitted optical power P for uniform and non-uniform OOK constellations are depicted in Fig. 3, assuming $\sigma_W^2 = 1$ and $\alpha = 1$, for the AWGN channel, the fast fading channel, and the block fading channel with $\epsilon = 10^{-2}$. Note that, by applying

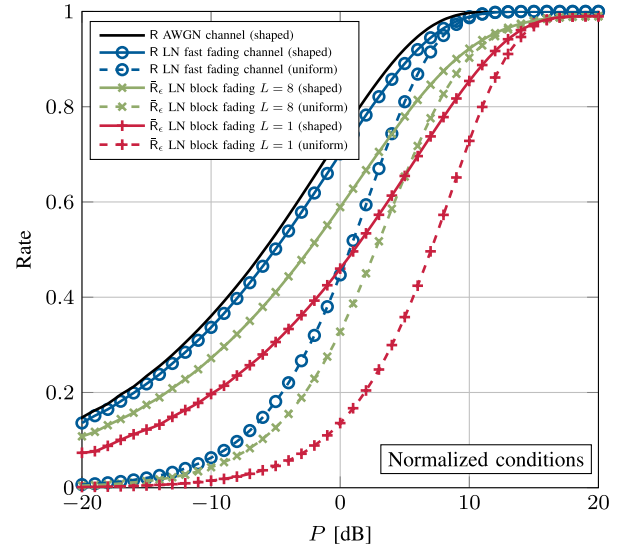


Fig. 3. Average rate in (18) for an IM/DD system: OOK transmission over AWGN, fast fading, and block fading channels; see text for parameters' values.

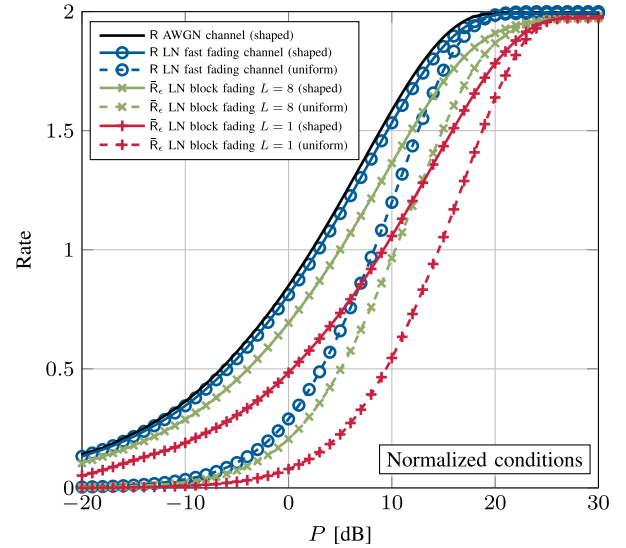


Fig. 4. Average rate in (18) for an IM/DD system: 4-ary transmission over AWGN, fast fading, and block fading channels; see text for parameters' values.

probabilistic shaping, i.e., by imposing a non-uniform distribution of the two input symbols, we get an increasing gain for decreasing P . Similarly, Fig. 4 shows the average rates $\bar{R}_{\epsilon, \text{IM/DD}}$ versus the average transmitted optical power P , for uniform and shaped 4-ary intensity modulation scheme with equally spaced constellation points, in the case of an AWGN channel, a fast fading channel, and a block fading channel with the same parameters as for the OOK case ($\sigma_W^2 = 1$, $\alpha = 1$, $\epsilon = 10^{-2}$). We point out that although probabilistic shaping can bring visible gains, its practical implementation for asymmetric (intensity) modulations comes with challenges. Usually, lower rates than those reported in Fig. 3 and in Fig. 4 are achieved. For a discussion, the reader is referred to [18] and the references therein.

B. Coherent Transmission System

For ease of presentation, we consider one dimension of the signal for analysis, i.e., the in-phase (or quadrature)

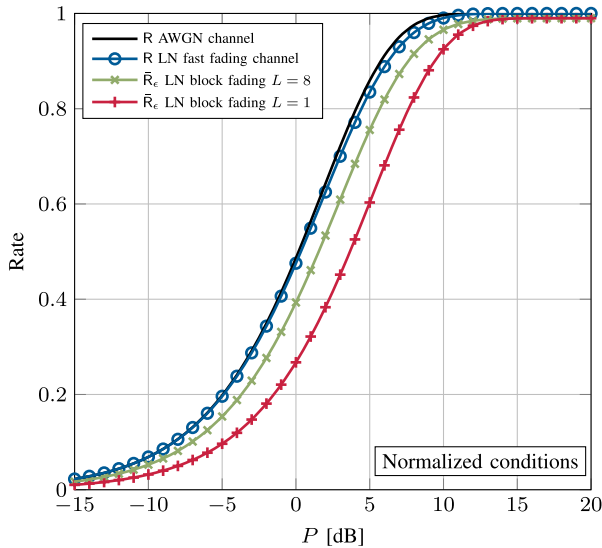


Fig. 5. Average rate in (24) for a coherent system: 2-ASK transmission over AWGN, fast fading, and block fading channels; see text for parameters' values.

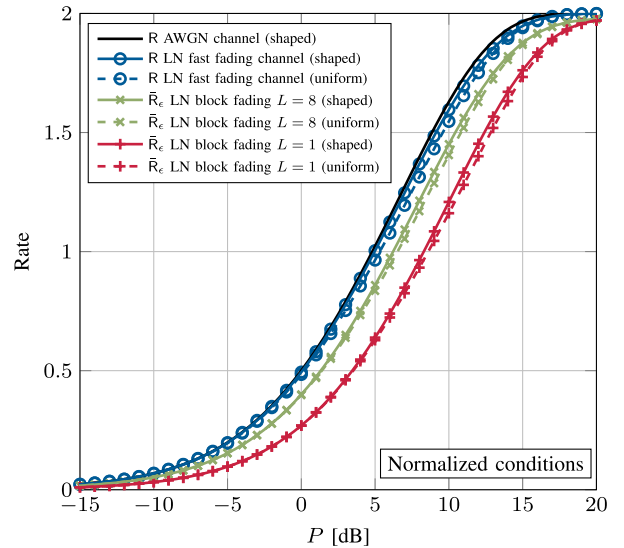


Fig. 6. Average rate in (24) for a coherent system: 4-ASK transmission over AWGN, fast fading, and block fading channels; see text for parameters' values.

component, hence only the corresponding noise component, with power $\sigma_W^2/2$, is accounted for. In the discrete-time system model in (4), the modulation symbol X is thus an M -ary ASK symbol (rather than a complex quadrature amplitude modulation (QAM) symbol). In a coherent transmission system, we impose a different normalization of the symbol constellation,

$$E[|X|^2] = 1, \quad (19)$$

so that the average transmitted optical power is $PE[|X|^2] = P$. As a consequence, for a given scintillation value $H = h$, the instantaneous SNR in (5) reduces to

$$\text{SNR}_{\text{coh}}(h) = \alpha h \frac{P}{\sigma_W^2/2}. \quad (20)$$

For an ergodic fading channel the capacity is

$$C_{\text{coh}} = \max_{P(x)} \int_0^\infty I(X; Y | H = h) p_h(h) dh \quad (21)$$

where the MI $I(X; Y | H = h)$ in (21) corresponds to the MI of an AWGN channel with instantaneous $\text{SNR}_{\text{coh}}(h)$.

For the block fading channels, similarly to the IM/DD case, we derive the outage probability as

$$p_{\text{out,coh}}(R) = \Pr \left\{ \max_{P(x)} \frac{1}{L} \sum_{\ell=1}^L I(X, Y, H_\ell) < R \right\} \quad (22)$$

where the r.v. $I(X, Y, H_\ell)$ is the rate supported in block ℓ with values $I(X; Y | H_\ell = h)$. The ϵ -outage capacity $C_{\epsilon, \text{coh}}$ for the block fading channel is then

$$C_{\epsilon, \text{coh}} = \underset{R}{\operatorname{argmax}} p_{\text{out,coh}}(R) < \epsilon. \quad (23)$$

In average, error-free communication is possible at a rate

$$\bar{R}_{\epsilon, \text{coh}} = (1 - \epsilon) C_{\epsilon, \text{coh}}. \quad (24)$$

Fig. 5 shows the average rates $\bar{R}_{\epsilon, \text{coh}}$ versus the average transmitted optical power P , assuming $\sigma_W^2/2 = 1$ and $\alpha = 1$, for a uniform input distribution 2-ASK, for an AWGN channel, a fast fading channel, and a block fading channel with $\epsilon = 10^{-2}$. Note that a uniform input distribution maximizes the rate for 2-ASK modulations. Similarly, for a 4-ary modulation scheme, Fig. 6 shows the average rates $\bar{R}_{\epsilon, \text{coh}}$ versus the average transmitted optical power P , still assuming normalized noise variance and non-random optical power loss ($\sigma_W^2/2 = 1$ and $\alpha = 1$), for uniform and shaped 4-ASK, again for an AWGN channel, a fast fading channel, and a block fading channel with $\epsilon = 10^{-2}$. Observe that shaping gains are limited for such low-order modulations over the lognormal fading channel. Nevertheless, for symmetric constellations, probabilistic shaping can be efficiently implemented by, e.g., relying on probabilistic amplitude shaping (PAS). As concern PAS, we use an outer shaping code concatenated with an inner systematic error correcting code. This way it is possible to generate a channel input alphabet characterized by the desired distribution. In practice, constant composition outer codes together with low-density parity-check (LDPC) inner codes can achieve rates close to capacity (see [19] for details).

IV. PERFORMANCE COMPARISON OF IM/DD AND COHERENT SYSTEMS

As discussed in Sec. II-D, the comparison between the performance of an IM/DD and a coherent system is based here on the average transmitted optical power, which appears as the independent variable in all the figures described above, that report the information rates and assess system performance. Therein, the variance of additive Gaussian noise (σ_W^2) has been normalized, and the sources of non-random attenuation (α) have been neglected.

In order to directly compare the information rates that are achievable by the two types of systems, receiver noise and channel attenuation should then be evaluated and accounted

TABLE I
LINK BUDGET FOR THE FSO LINK, CONSIDERING DIFFERENT SECTORS OF THE ELEVATION ANGLES

sector number	1	2	3	4	5	6
elevation range (°)	5-7	7-10	10-15	15-22	22-37	37-90
satellite altitude (km)	693	693	693	693	693	693
link range (km)	2546.9	2372.8	2139.9	1819.8	1487.4	1066
Tx optical loss (dB)	3	3	3	3	3	3
Tx aperture (cm)	5	5	5	5	5	5
Tx antenna gain (dB)	99.2	99.2	99.2	99.2	99.2	99.2
Free space loss (dB)	266.3	265.7	264.8	263.4	261.6	258.7
atmospheric attenuation (dB)	2.6	1.9	1.4	0.9	0.6	0.4
cloud margin (dB)	3	3	3	3	3	3
Rx aperture (cm)	40	40	40	40	40	40
Rx antenna gain (dB)	117.1	117.1	117.1	117.1	117.1	117.1
Rx optical loss (dB)	3	3	3	3	3	3
Total optical power loss α^{-1} (dB)	61.6	60.3	58.9	57.0	54.9	51.8

for. Fortunately, this is feasible in an a-posteriori way, thanks to the fact that the systems in (1) and (4) are modelled as additive Gaussian channels.

In order to compute the link budget, we report in Table I the main channel parameters that determine the optical power loss α^{-1} , reported in dB in the last row of the Table. Since the FSO channel characteristics strongly depend on the elevation angle under which the ground station sees the satellite, we have divided the satellite pass in six angular sectors. The angular range of each sector is reported in Table I.⁶

Regarding the receiver parameters, Table II reports some typical values for an IM/DD receiver⁷ or for a preamplified coherent receiver. We assume a symbol rate equal to 10 GBd, hence the (one-sided) bandwidth of the receiver is set equal to half the symbol rate, i.e., $\Delta f = 5$ GHz, as also results in the IM/DD case where, by a simple single-pole approximation we obtain $(2\pi R_L C_L)^{-1} \simeq 5$ GHz. This, in turn, yields the variance of thermal noise (26) and that of the (single-polarization) input ASE noise, from (40), whose values are reported in Table II.

Results in Secs. III-A and III-B were plotted versus normalized abscissas, where $\sigma_W^2 = 1$ was set in the IM/DD case and $\sigma_W^2/2 = 1$ in the coherent case; in addition, $\alpha = 1$ was assumed. Therefore, when comparing corresponding curves, e.g., in Fig. 3 and Fig. 5, the different noise variance, as well as the common loss α^{-1} must be accounted for. To this aim, the normalized abscissa P used in Sec. III must be scaled to include both effects. Thus, the resulting average transmitted optical power P is computed from eqs. (20) and (14), for IM/DD and coherent systems, respectively, under *real* conditions, i.e., with values of α and σ_W^2 derived from the parameters in Tables I and II. Graphically, this means that the curve from the IM/DD system must be shifted to the left by $10 \log_{10}(\alpha/\sigma_W)$ and that of the coherent system must be shifted to the left by $10 \log_{10}((2\alpha)/\sigma_W^2)$.

⁶The values in Table I are consistent with those reported in Table III in [2].

⁷These values are also consistent with those reported in [2].

TABLE II
RECEIVER PARAMETERS AND RESULTING NOISE VARIANCE, FOR IM/DD AND PREAMPLIFIED COHERENT RECEIVERS

Parameter	Value
Responsivity R_d	1.0 A/W
Load+Feedback resistance R_L	160 Ω
Load+Feedback capacitance C_L	0.2 pF
Temperature T_0	290 K
Thermal Noise variance σ_T^2	-123.0 dB
receiver bandwidth Δf	5 GHz
Amplifier Gain G	23 dB
Carrier wavelength λ_0	1550 nm
Spontaneous emission factor n_{sp}	1.75
Input ASE Noise variance $\sigma_{ASE}^2/(2G)$	-89.5 dB

To give an example, assume the most favorable FSO channel characteristics, with an elevation angle between 37 and 90 degrees, corresponding to ‘sector 6’ in Table I, where the link budget yields a total optical power loss amounting to $\alpha^{-1} = 51.8$ (dB). Fig. 7 shows the comparison between an IM/DD and a coherent system, by considering binary transmission over the AWGN channel, with OOK and 2-ASK modulations in the two cases, respectively. Therein, the curve for the IM/DD case is obtained by shifting the corresponding curve in Fig. 3 to the left by $10 \log_{10}(\alpha/\sigma_W) = 9.7$ dB, where we used the value in the last column of Table I for the total optical power loss and the value in Table II for the thermal noise variance. Similarly, the curve for the coherent case in Fig. 7 is obtained by shifting the corresponding curve in Fig. 5 to the left by $10 \log_{10}(2\alpha/\sigma_W^2) = 40.7$ dB, where the values of α and that of the ASE noise variance $\sigma_W^2 = \sigma_{ASE}^2/(2G)$ are again taken from Table I (last column) and Table II.

As another example, Fig. 8 compares an IM/DD and a coherent system, by considering transmission over a fast fading channel, with 4-ary symbol constellations assuming probabilistic shaping. The FSO channel with an elevation

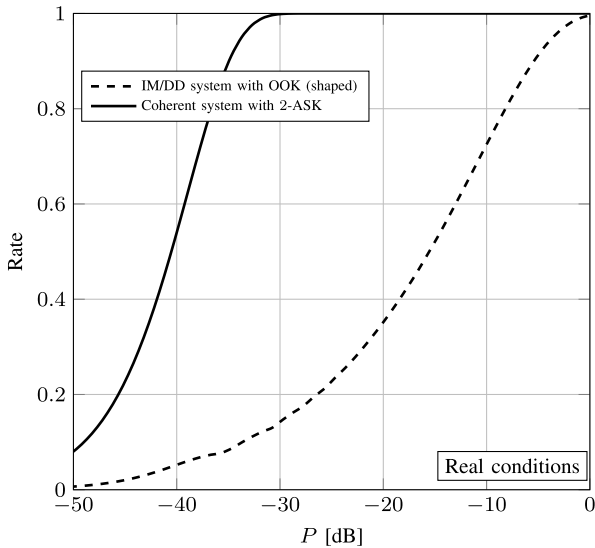


Fig. 7. Comparison of IM/DD and coherent systems, transmitting binary symbols over the AWGN channel in the most favorable FSO channel conditions ('sector 6').

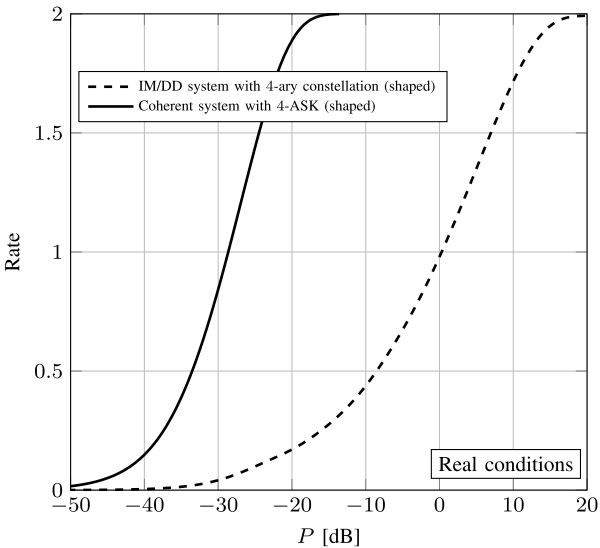


Fig. 8. Comparison of IM/DD and coherent systems, transmitting 4-ary symbols over the LN fast fading channel for elevations between 10 and 15 degrees ('sector 3').

angle between 10 and 15 degrees ('sector 3') is chosen, where the total optical power loss in Table I is $\alpha^{-1} = 58.9$ dB. The curves in Fig. 8 are obtained from the corresponding ones in Fig. 4 and Fig. 6, for the IM/DD and coherent systems, respectively. In the two cases, the shifts to the left are computed as $10 \log_{10}(\alpha/\sigma_W) = 2.6$ dB, for the IM/DD system, and as $10 \log_{10}(2\alpha/\sigma_W^2) = 33.6$ dB, for the coherent system. Again, the values in Table I (third column) and Table II were used for the total optical power loss and for the thermal or ASE noise variance.

As evident from the system comparisons described above, accounting for the optical power loss and noise variance changes completely the trend that appears from the Figures in Secs. III-A and III-B. While channel attenuation is common to both kinds of systems, the impact of noise is very different

due to their profound technological differences. In particular, in computing the above shifts for the curves in Fig. 7 and Fig. 8, note that the presence of a square power on the coherent case only is not a contradiction but, rather, is the very consequence of the different system models in (1) and (4), where the different technological solutions imply different costs, that are not accounted for in the comparison. Recall also that for the coherent setup, the transmission rates can in principle be increased by a factor of four when accounting for the quadrature component and dual polarization.

V. CONCLUSION AND FURTHER RESEARCH

We evaluated the information rates of two FSO communication systems impaired by atmospheric turbulence, for both ergodic fading and block fading channels. In the presence of the same transmission medium, the two systems adopt a coherent or a more traditional IM/DD transceiver, respectively. The average transmitted optical power was considered to be the main resource, especially in a LEO satellite downlink, that we considered for comparing the two systems.

Relying on simple but meaningful channel models, we highlighted how the physical channel parameters (i.e., the optical power loss and the random fading due to turbulence), as well as the transceiver parameters (i.e., the transmitted optical power, the symbol constellation and the receiver noise) affect the two types of systems in different ways. In particular, the profound technological difference between the two solutions implies that receiver noise stems from physically different sources and reaches very different levels, for typical system parameters, giving a clear advantage to the more costly and performing coherent system, even when polarization multiplexing is not exploited.

The value of the proposed method lies in the possibility to quantify the gain that the coherent solution can achieve, and compare it against the higher cost that it implies. The comparison should thus be performed on a techno-economical basis, that goes beyond the scope of this work. Another result that we found is that a significant shaping gain can be achieved for OOK modulation in an IM/DD system. In addition, for the block-fading channel model, we also quantified the gain in performance that can be achieved through an increased diversity order.

A possible extension of this work can be the evaluation of system performance, in terms of achievable information rates, where a peak-power constraint is considered, in addition to the one on average power. In this case, the theoretical result (11) does not hold anymore and the analysis in [20], performed for a coherent channel, shows that the capacity-achieving input distribution is a finite and discrete set of signal values (that are not easy to express in closed form). A further extension of this work can consider different probabilistic scintillation models, such as the gamma-gamma distribution, which is an appropriate choice for moderate to large scintillation indices.

APPENDIX A

SOURCES OF NOISE IN OPTICAL RECEIVERS

The receiver design for optical transmission systems has undergone several paradigmatic changes through the last

decades, depending on many factors, including the available technologies, the level of optical signal power that is detected on average, and the field of application, along with modulation techniques, in the case of telecommunications. Each of the design paradigms has its sources of noise that impair the received signal, among which one has to select the dominant one in order to evaluate the SNR affordably and devise the best way to process the signal after opto-electronic and analog-to-digital conversions. Basically, we can classify optical receivers in two large families: those based on positive intrinsic negative (PIN) diodes or APDs and those including an optical amplifier, followed either by a simple photodetector (usually a PIN, since the extra gain provided by APDs is not necessary) or by a more sophisticated coherent detector (including 90°-hybrids and balanced photodiodes), in which case optical preamplification is a mandatory solution, unless the received signal is powerful enough.

Albeit in this work we consider optical preamplification only in the presence of coherent O/E conversion, we briefly describe the sources of noise that can arise in different receiver configurations.

A. Direct Detection (APD) Receiver With Electronic Amplification

even assuming an ideal receiver, the quantum nature of light is such that the detection of lightwave signals includes the photon detection quantum noise, with Poisson statistics, i.e., the so-called shot-noise, that is obviously signal dependent. No matter if a photodiode is inversely polarized on a simple bias resistance or is inserted in a more complicated circuit with electronic amplification (such as a TIA), thermal noise is also introduced by the electronic components, which is signal-independent and is usually assumed to dominate over shot noise, unless the received photon flux is extremely weak (and the granularity of photon arrivals cannot be neglected). The dominance of thermal noise allows to study the optical transmission system in the classical framework of additive signal-independent Gaussian noise. However, shot noise comes back into play when APDs are used, because of their statistical gain fluctuation, which must be taken into account by an excess noise factor.

Assuming that the received optical field E_s is detected by a photodiode with responsivity $R_d = \frac{\eta q}{h\nu_0}$ (where η is the quantum efficiency at the carrier wavelength ν_0 , q is the electron charge and h the Planck's constant), the output photocurrent is

$$I = R_d P_s + i_s + i_T \quad (25)$$

where $P_s = |E_s|^2$ is the received signal power and the dependence on time is omitted for brevity. In (25), i_T and i_s are thermal and shot noise, whose variances, as computed on the signal bandwidth Δf , are

$$\sigma_T^2 = \frac{4kT_0}{R_L} \Delta f \quad (26)$$

$$\sigma_s^2 = 2qR_d P_s \Delta f \quad (27)$$

k being Boltzmann's constant, T_0 the receiver temperature, and R_L its load resistance. The resulting electrical SNR is

$$SNR_e^{sT} = \frac{R_d^2 P_s^2}{\sigma_s^2 + \sigma_T^2} \quad (28)$$

$$SNR_e^s \simeq \frac{P_s}{2h\nu_0 \Delta f} \quad (29)$$

where the second expression results by neglecting thermal noise (i.e., for a shot-noise limited receiver) and assuming an ideal quantum efficiency $\eta = 1$. Beside thermal and shot noise, other minor noise sources, like the bulk dark current and the surface leakage current of photodiodes, could be considered but are usually neglected, as is the ambient light noise.

B. Optically Preamplified Direct Detection Receiver

a completely different scenario is opened up by the introduction of optical preamplification, since an optical amplifier (let it be an erbium doped fiber amplifier (EDFA) which is the most common choice) introduces a gain G on the receive optical power, at the cost of ASE noise $E_{ASE} = E_{\parallel} + E_{\perp}$ that is added on the top of the electric field, so that, after direct detection, the output photocurrent becomes

$$\begin{aligned} I &= R_d \left(|\sqrt{G}E_s + E_{\parallel}|^2 + |E_{\perp}|^2 \right) + i_s + i_T \\ &= R_d G P_s + i_{s-ASE} + i_{ASE-ASE} + i_s + i_T. \end{aligned} \quad (30)$$

The ASE noise field in (30) is split in two orthogonally polarized components (with equal average power), one of them, E_{\parallel} , being parallel to that of the signal field E_s while the other, E_{\perp} , is orthogonal to it. As evident in (30), the signal is added only to the parallel component, in the photodetection process, which gives rise to the so-called signal-ASE beat noise i_{s-ASE} , whose average value is zero since the noise current rapidly fluctuates in time and is not coherent (neither in frequency nor in phase) with the signal. The mean square value of i_{s-ASE} , i.e., its variance, is however nonzero and can be expressed as

$$\sigma_{s-ASE}^2 = 4R_d^2 G P_s (S_{ASE}/2) \Delta f \quad (31)$$

where S_{ASE} is the power spectral density of ASE noise, that can be evaluated after a quantum description of the spontaneous emission process occurring in multiband excited ions (Erbium, in this case) as

$$S_{ASE} = 2 n_{sp} h\nu_0 (G - 1), \quad (32)$$

where n_{sp} is the spontaneous emission factor, also known as population inversion factor, with typical values $1.5 \div 2$, and the factor 2 accounts for the two optical polarizations cited above, with which a photon can be spontaneously emitted. From (32), the average of the ASE-ASE beat noise current $i_{ASE-ASE}$ in (30), as well as its variance, can be calculated as

$$\begin{aligned} \langle i_{ASE-ASE} \rangle &= R_d S_{ASE} \Delta f_{ASE} \\ \sigma_{ASE-ASE}^2 &= R_d^2 G S_{ASE}^2 \Delta f (\Delta f_{ASE} - \Delta f/2), \end{aligned} \quad (33)$$

where Δf_{ASE} is the overall bandwidth of ASE noise, which is usually limited by placing an optical filter, with a bandwidth

equal to that of the useful signal, right after the optical amplifier. Due to the presence of ASE noise, the expression of the photodetected current as well as that of shot noise must be modified to account for it, so that (27) becomes

$$\sigma_s^2 = 2qR_d(GP_s + S_{ASE}\Delta f_{ASE})\Delta f \quad (34)$$

and the resulting electrical SNR is

$$\begin{aligned} SNR_e^{AsT} &= \frac{R_d^2(GP_s + S_{ASE}\Delta f_{ASE})^2}{\sigma_{s-ASE}^2 + \sigma_{ASE-ASE}^2 + \sigma_s^2 + \sigma_T^2} \\ &\simeq \frac{R_d^2 G^2 P_s^2}{\sigma_{s-ASE}^2 + \sigma_s^2 + \sigma_T^2} \end{aligned} \quad (35)$$

where the second expression comes from neglecting the ASE-ASE beat term, which is negligible in the case of a sufficiently large signal power that makes the signal-ASE term the dominant one. If thermal noise can be further neglected compared to shot noise, we can again use the approximation in (29) to write

$$SNR_e^{As} \simeq \frac{GP_s}{(2S_{ASE} + 2h\nu_0)\Delta f}. \quad (36)$$

By comparing (29) and (36), we find a counter-intuitive result, such that the introduction of optical amplification degrades the SNR by an amount equal to the noise figure

$$F = \frac{SNR_e^{As}}{SNR_e^{As}} = 2 n_{sp} \left(1 - \frac{1}{G}\right) + \frac{1}{G} \simeq 2 n_{sp} > 1. \quad (37)$$

The above conclusion, however, does not have a practical value, since it is often the thermal noise that dominates over shot noise. Indeed, optical amplification is introduced to combat the additive thermal noise and make it negligible compared to the dominant source of noise, that is the signal-ASE beat. In fact, considering the SNR in (28) with only thermal noise and that in (35) with signal-ASE as well as thermal noise, the ratio

$$\frac{SNR_e^{AT}}{SNR_e^T} = \frac{G\sigma_T^2}{R_d^2 P_s (\sigma_T^2 + 2S_{ASE}\Delta f)} \quad (38)$$

can be thought of as being very large, especially in the case of a weak signal (small P_s) subject to a strong amplification (large G).

In the end, for a typical optically preamplified direct detection receiver, we can safely assume that the signal-ASE beat term is the dominant source of noise and that the resulting electrical SNR is well approximated as

$$SNR_e \simeq SNR_e^A = \frac{GP_s}{4n_{sp}h\nu_0(G-1)\Delta f}. \quad (39)$$

C. Optically Preamplified Coherent Receiver

significantly, the expression in (39) is in all respects similar to the electrical SNR that is evaluated at the output of an optically preamplified coherent receiver, where (different from (30)) the received electric current is $I = \sqrt{GE_s} + E_{\parallel} + E_{\perp}$, after a direct opto-electronic conversion of the received optical field, including both the useful signal and the ASE noise. Thus, the power of the signal component is simply GP_s while that of the ASE noise,

$$\sigma_{ASE}^2 = 2 n_{sp} h\nu_0 (G-1) \Delta f, \quad (40)$$

is obtained by integrating the white power spectral density (32) over the signal bandwidth Δf . If one assumes that the ASE component E_{\perp} orthogonal to the signal polarization is filtered out (an ideal operation, that is far from being easily accomplished in practice), then the ASE noise variance is halved and the corresponding SNR, considered at the amplifier input, can be expressed as

$$SNR_e^{\text{coh}} = \frac{P_s}{n_{sp} h\nu_0 (1 - 1/G) \Delta f}, \quad (41)$$

which corresponds to the expression (5), where the optical power at the preamplifier input is $P_s = \alpha h P E \left[|X|^2\right]$, obtained for the system that we analyze in Sec. II-B.

ACKNOWLEDGMENT

This work has been supported by European Space Agency (ESA) funded activity SatNEx V COO2 WI 2.3 ‘‘Fibre optics techniques for future free-space optical satellite communications.’’ The views of the authors of this paper do not necessarily reflect the views of ESA.

REFERENCES

- [1] J. M. Kahn and J. R. Barry, ‘‘Wireless infrared communications,’’ *Proc. IEEE*, vol. 85, no. 2, pp. 265–298, Feb. 1997.
- [2] P.-D. Arapoglou, G. Colavolpe, T. Foggi, N. Mazzali, and A. Vannucci, ‘‘Variable data rate architectures in optical LEO direct-to-earth links: Design aspects and system analysis,’’ *J. Lightw. Technol.*, vol. 40, no. 16, pp. 5541–5556, Aug. 15, 2022.
- [3] G. Colavolpe, T. Foggi, and A. Vannucci, ‘‘Synchronization for variable data rate LEO direct-to-earth optical links,’’ in *Proc. IEEE Int. Conf. Commun.*, May 2022, pp. 3064–3069.
- [4] K. Riesing et al., ‘‘Operations and results from the 200 Gbps TBIRD laser communication mission,’’ in *Proc. 37th Annu. Small Satell. Conf. (SSC)*. Logan, UT, USA: Utah State Univ., 2023, pp. 1–3.
- [5] B. Edwards, D. Antsos, A. Biswas, L. Braatz, and B. Robinson, ‘‘An envisioned future for space optical communications,’’ in *Proc. IEEE Int. Conf. Space Opt. Syst. Appl. (ICSOS)*, Vancouver, BC, Canada, Jun. 2023, pp. 1–7.
- [6] A. A. Farid and S. Hranilovic, ‘‘Channel capacity and non-uniform signalling for free-space optical intensity channels,’’ *IEEE J. Sel. Areas Commun.*, vol. 27, no. 9, pp. 1553–1563, Dec. 2009.
- [7] L. Paillier, R. Le Bidan, J.-M. Conan, G. Artaud, N. Védrenne, and Y. Jaouën, ‘‘Space-ground coherent optical links: Ground receiver performance with adaptive optics and digital phase-locked loop,’’ *J. Lightw. Technol.*, vol. 38, no. 20, pp. 5716–5727, Oct. 15, 2020.
- [8] D. Dravins, L. Lindgren, E. Mezey, and A. T. Young, ‘‘Atmospheric intensity scintillation of stars, I. Statistical distributions and temporal properties,’’ *Publications Astronomical Soc. Pacific*, vol. 109, p. 173, Feb. 1997, doi: 10.1086/133872.
- [9] M. L. B. Riediger, R. Schober, and L. Lampe, ‘‘Fast multiple-symbol detection for free-space optical communications,’’ *IEEE Trans. Commun.*, vol. 57, no. 4, pp. 1119–1128, Apr. 2009.
- [10] A. Vannucci et al., ‘‘From fibers to satellites: Lessons to learn and pitfalls to avoid when optical communications move to long distance free space,’’ in *Proc. 56th Asilomar Conf. Signals, Syst., Comput.*, Oct. 2022, pp. 888–893.
- [11] A. Belmonte and J. M. Kahn, ‘‘Satellite downlink coherent laser communications,’’ in *Optical Wireless Communications*. Berlin, Germany: Springer, 2016, pp. 325–343.
- [12] M. Shtaif, C. Antonelli, A. Mecozzi, and X. Chen, ‘‘Challenges in estimating the information capacity of the fiber-optic channel,’’ *Proc. IEEE*, vol. 110, no. 11, pp. 1655–1678, Nov. 2022.
- [13] L. G. Kazowsky, S. Benedetto, and A. Willner, *Optical Fiber Communication*. Norwood, MA, USA: Artech House, 1996.
- [14] R. Barrios, B. Matuz, and R. Mata-Calvo, *Satellite Communications in the 5G Era*, S. K. Sharma, S. Chatzinotas and P. Arapoglou, Eds. London, U.K.: IET, 2018, ch. 12, pp. 341–373.

- [15] M. Secondini and E. Forestieri, "Scope and limitations of the nonlinear Shannon limit," *J. Lightw. Technol.*, vol. 35, no. 4, pp. 893–902, Feb. 15, 2017.
- [16] M. Secondini, "Information capacity of optical channels," in *Optical Fiber Telecommunications VII*, A. E. Willner, Ed. New York, NY, USA: Academic, 2020, pp. 867–920. [Online]. Available: <https://www.sciencedirect.com/science/article/pii/B9780128165027000233>
- [17] P. J. Winzer, "Transmission system capacity scaling through space-division multiplexing: A techno-economic perspective," in *Optical Fiber Telecommunications VII*, A. E. Willner, Ed. New York, NY, USA: Academic, 2020, pp. 337–369. [Online]. Available: <https://www.sciencedirect.com/science/article/pii/B9780128165027000099>
- [18] T. Wiegart, L. Wang, D. Lentner, and R. D. Wesel, "Probabilistic shaping for asymmetric channels and low-density parity-check codes," in *Proc. 12th Int. Symp. Topics Coding (ISTC)*, Brest, France, Sep. 2023, pp. 1–5.
- [19] G. Böcherer, P. Schulte, and F. Steiner, "Bandwidth efficient and rate-matched low-density parity-check coded modulation," *IEEE Trans. Commun.*, vol. 63, no. 12, pp. 4651–4665, Dec. 2015.
- [20] J. G. Smith, "The information capacity of amplitude- and variance-constrained scalar Gaussian channels," *Inf. Control*, vol. 18, no. 3, pp. 203–219, Apr. 1971. [Online]. Available: <https://www.sciencedirect.com/science/article/pii/S001995871903469>

Ayman Zahn (Graduate Student Member, IEEE) received the B.S. degree (cum laude) in computer, electronic and communication engineering and the M.Sc. degree (cum laude) in communication engineering from the University of Parma, Parma, Italy, in 2017 and 2020, respectively. He is currently pursuing the Ph.D. degree with the Institute for Communications Engineering, Technical University of Munich, Munich, Germany. His main research interests include digital communication systems, channel coding, and information theory.

Giulio Colavolpe (Senior Member, IEEE) received the Dr.-Ing. degree (cum laude) in telecommunications engineering from the University of Pisa, Italy, in 1994, and the Ph.D. degree in information technologies from the University of Parma, Italy, in 1998. Since 1997, he has been with the University of Parma, where he is currently a Professor of telecommunications with the Dipartimento di Ingegneria e Architettura (DIA). In 2000, he was a Visiting Scientist with the Institut Eurécom, Valbonne, France. In 2013, he was a Visiting Scientist with the European Space Agency (ESTEC), Noordwijk, The Netherlands. His research activity has led to more than 200 articles in refereed journals, leading international conferences, and 18 industrial patents. His research interests include the design of digital communication systems, adaptive signal processing (with particular emphasis on iterative detection techniques for channels with memory), and channel coding and information theory. He received the Best Paper Award from the 13th International Conference on Software, Telecommunications and Computer Networks (SoftCOM 2005), Split, Croatia, in September 2005; the Best Paper Award for Optical Networks and Systems from the IEEE International Conference on Communications (ICC 2008), Beijing, China, in May 2008; and the Best Paper Award from the Fifth Advanced Satellite Mobile Systems Conference and the 11th International Workshop on Signal Processing for Space Communications (ASMS&SPSC 2010), Cagliari, Italy. He served as an Editor for IEEE TRANSACTIONS ON WIRELESS COMMUNICATIONS, the IEEE TRANSACTIONS ON COMMUNICATIONS, and IEEE WIRELESS COMMUNICATIONS LETTERS; and an Executive Editor for *Transactions on Emerging Telecommunications Technologies (ETT)*.

Tommaso Foggi received the master's degree in telecommunication engineering and the Ph.D. degree in information technology from the University of Parma, Italy, in 2003 and 2008, respectively. From 2009 to 2018, he was a Research Engineer with the National Inter-University Consortium for Telecommunications (CNIT), University of Parma Research Unit. He is currently an Associate Professor with the Department of Engineering and Architecture, University of Parma. He is the author of tens of peer-reviewed articles and several patents. His main research interests include electronic signal processing for optical and satellite communication systems. He won the Best Paper Award in Optical Networks and Systems from the IEEE International Conference on Communications (ICC 2008), Beijing, China, in May 2008. He was/is involved in many research projects funded by public authorities, such as MIUR, ESA, and EU or private companies, such as Ericsson, CGS, Inmarsat, and Huawei.

Balázs Matuz (Senior Member, IEEE) was born in Budapest, Hungary, in 1982. He received the Diploma degree in electrical engineering and information technology from Technische Universität München (TUM) in 2007 and the Ph.D. degree (Hons.) from Technische Universität Hamburg-Harburg (TUHH) in 2013. Since 2007, he has been a member of the Scientific Staff of the German Aerospace Center (DLR), Germany. He further visited the University of Parma, Italy, the University of Dalhousie, Canada, the University of Sydney, Australia, and the University of Newcastle, Australia, in the framework of international exchange programs. In 2012, he spent a sabbatical term with the University of Bologna, Italy, as a recipient of the DLR Research Semester Grant. Since 2014, he has been a Guest Lecturer with TUM. During the past years, he has been involved in several national and international projects on this subject. Amongst others, he participated in the development of a DVB-SH prototype system. Likewise, he has been involved in several standardization activities, amongst others in the framework of the consultative committee for space data systems (CCSDS) or the 5th generation mobile networks (5G) standardization. His research interests include novel channel coding and signal-processing techniques for terrestrial and space communications. He serves as a technical program committee member and a reviewer for transactions, journals, and conferences. From 2018 to 2023, he was an Associate Editor of IEEE COMMUNICATION LETTERS.

Armando Vannucci received the Dr.-Ing. degree (cum laude) in electronic engineering from the University of Rome "La Sapienza" in 1993, with a focus on digital analysis of speech signals applied to speech recognition, and the Ph.D. degree in information technology from the University of Rome, Rome, Italy, in 1998. From 1993 to 1994, he was with the Department of INFO-COM, University of Rome. From 1995 to 1998, as a Ph.D. Student, he joined an industrial research project on digital radio links, for which he holds two patents with the University of Parma, discussing the thesis "Sequence Estimation Receivers for Nonlinear Transmission Channels" with the Polytechnic of Turin. From 1998 to 2002, he held various positions at the University of Parma, where he became an Assistant Professor in 2002. His research interests include variational techniques for the design of digital receivers, fiber optics transmission, polarization mode dispersion, optical amplifiers, and digital speech processing. He took part in various research projects, both institutional and with industrial partners. He is the author of more than 50 scientific publications, mostly in international journals (40%), conference proceedings, books, book chapters, and patents. He was a Visiting Scientist with Alcatel Labs, Marcoussis, France, and with Université Laval, Québec City, QC, Canada, and a Visiting Lecturer with Hochschule Karlsruhe, Germany. He is the author of two textbooks and has taught several courses (undergraduate, graduate, master, Ph.D., and summer schools) with the Universities of Rome, Urbino, and Parma, where he is currently In-charge of signals and systems.